RESEARCH PAPER

Carbon-nanotube-based electrically-short resonant antennas

PIERRE FRANCK[1,2], DOMINIQUE BAILLARGEAT[1,2] AND BENG KANG TAY[1,3]

We present a study on using carbon nanotubes (CNTs) as the radiating part of resonant antennas in order to reduce their dimensions. A mesoscopic electromagnetic (EM) model for CNTs was developed to allow the simulation of RF devices in classical EM solvers while retaining the specific properties of CNTs. A circuit approach is also used to provide a physical interpretation of the results on monopole antennas and trend prediction. These techniques constitute a platform to study the trends and trade-offs involved in the design of these antennas. Finally, these results are used to assess suitable fabrication techniques for CNT-based short resonant antennas and conclusions are drawn on their potential applications.

I. INTRODUCTION

As device manufacturers try and maintain Moore's law, the physical limits of usual techniques and materials in electronics become more and more difficult to circumvent. Great hopes lie in the use of new materials, such as carbon nanotubes (CNTs) or graphene. They present a high conductivity, resistance to electromigration, fast time response. However, efforts have mainly been focused on realizing CNT components such as field-effect transistors (FETs) or sensors often overlooking their connection to more conventional electronics. Those devices are intrinsically small and high-impedance and metal-CNT contacts are still to date high-resistance and difficult to reproduce. A wireless connection to these components would be highly beneficial by remediating to problems of high-precision contacting and impedance matching especially if the same CNTs can be used to accomplish the component function and to radiate.

When applied to the case of antennas, CNTs could also help miniaturization from a different perspective. In fact, the ever increasing needs in connectivity and high data rate for portable devices equate with the integration of multiple antennas with a non-negligible footprint. Antennas need to be resonant to offer good radiation performance, which sets a minimum length of about a quarter wavelength at nominal frequency – centimeters for Wi-Fi. However, CNTs present a high kinetic inductance [1] that results on slow-wave

propagation along their axis and thus a resonant antenna size reduction of up to 50 [1, 2].

II. CNT MODELLING

A) Models

We rely on two complementary approaches to model CNTs integrated in electronic components. Firstly, a circuit approach, derived from [1, 3, 4], secondly, an electromagnetic (EM) approach [5] based on [6]. These models are inherently limited to the case of metallic single-wall carbon nanotubes (m-SWCNTs) of limited diameter ($a_{max} = 6.8$ nm) studied at frequencies up to 30 THz – below interband transition regime [6, 7]. In these conditions, semiconducting CNTs contribution can be neglected as their conductivity is 2 to several orders of magnitude smaller than that of the metallic ones [6] and both species are typically present in similar quantities in unsorted CNTs. There exist appropriate models [7, 8] to deal with the cases that exceed these limits and they can be implemented following the same approaches. However, the current description is focused on the most interesting case for antennas. Indeed, kinetic inductance decreases with increasing CNT diameter and number of shells [8] thus lessening the shortening effect we seek by using CNTs in antennas.

The circuit model relies on a transmission line approach where the traditional electrostatic capacitance, magnetic inductance and resistance are completed with a kinetic inductance – predominant in CNTs – and a quantum capacitance [3, 4]. Once derived, a circuit model allows quick analysis of simple structures and we use it to make physical sense of our results on monopole and dipole antennas. Nonetheless, in the case of most realistic antennas or to study radiation and feed structures, a three-dimensional (3D) EM simulation is necessary. The available EM model for CNTs was however

[1]CINTRA CNRS/NTU/THALES, UMI 3288, Research Techno Plaza, 50 Nanyang Drive, Border X Block, Level 6, Singapore 637553, Singapore. Phone: +6590870567
[2]XLIM UMR 7252, Université de Limoges/CNRS, 123 Avenue Albert Thomas, 87060 Limoges, France
[3]School of Electrical and Electronics Engineering, Nanyang Technological University, Block S1, 50 Nanyang Avenue, Singapore 639798, Singapore
Corresponding author:
P. Franck
Email: pierre.franck@xlim.fr

57

incompatible with finite-element analysis of more than a few CNTs. It describes each CNT as a shell with given surface conductivity [2, 6], which makes it extremely difficult to mesh and solve because of the many scales involved. CNT diameters are in the 0.1–6.8 nm range, CNT lengths and microelectronic components in the 0.1–1000 μm range and there can be anywhere between a single CNT and billions of CNTs.

To address this matter we have developed a mesoscopic model based on an effective medium approach and the model in [6]. SWCNTs are modeled using a material with anisotropic complex EM properties as originally described in [5]. We use published values for the phenomenological constants. The complex conductivity of an array of CNTs aligned along the z-axis in Cartesian coordinates can be written:

$$\begin{pmatrix} \sigma_T & 0 & 0 \\ 0 & \sigma_T & 0 \\ 0 & 0 & \sigma_{Axial} \end{pmatrix}, \qquad (1)$$

where σ_T is the transverse conductivity and σ_{Axial} the axial conductivity. In the cases studied here the aligned CNTs are excited in common mode, separated by a dielectric, and their lateral spacing is large enough to prevent CNT-to-CNT transverse conductivity as defined in [5]. Hence, $\sigma_T = 0$ and, for a cross-sectional CNT density D_{NT}, the complex axial conductivity is:

$$\sigma_{Axial} = \sigma_{lin,0} \, D_{NT} \, \zeta(u), \qquad (2)$$

where

$$\sigma_{lin,0} = \frac{8e^2 v_F}{hv} = \frac{24e^2 b\pi}{h^2} \frac{\gamma_0}{v} = A\gamma_0\tau \qquad (3)$$

is the DC linear conductivity over a single SWCNT. It is linearly dependent on the phenomenological values γ_0 and $\tau = v^{-1}$, the overlap integral in the tight-binding description and the plasmon lifetime in the SWCNTs used, and taken to be 3 eV and 3 ps respectively for the numerical applications in this paper. The complex frequency dispersion profile and the normalized frequency are respectively:

$$\zeta(u) \equiv \frac{1 - ju}{1 + u^2}, \quad u \equiv \frac{\omega}{v} = \frac{f}{F_v}. \qquad (4)$$

Note that the conductivity is predominantly complex only for $f > F_v = 1/2\pi\tau = 53$ GHz for the chosen value of τ which is for excellent CNT quality. The quality of the CNTs used is thus a prime concern to ensure the feasibility of resonant antennas.

B) Implementation

The circuit model can be used to derive analytical formulas, which allow a better understanding of a structure. In the case of monopole and dipole structures we have derived and implemented these formulas in an Excel sheet to allow direct comparison with the EM results, further study of the trade-offs we will outline in the following sections and performance prediction before additional EM simulation [9]. The circuit model can also be implemented in Agilent's ADS [10] for more complicated structures.

The EM model is implemented in HFSS (Ansys) and EMXD (developed by Michel Aubourg at XLIM) – two frequency-domain 3D EM solvers both based on the finite-elements method. The implementation in EMXD allowed the validation of the model thanks to a point-by-point definition of the mesh in the open-source mesh generator GMSH and to non-ambiguous definition of complex conductivity in EMXD. HFSS, as a commercial distribution, is more widely available and a more versatile simulation suite.

It is then possible to select CNTs among other conventional materials while keeping control over the model parameters. This modeling approach has been validated by direct comparison with published theoretical and experimental results [2, 11]. Its equivalence to the model it is derived from (individual hollow tubes) has been demonstrated (cf. Fig. 1) while considerably cutting the simulation time and required memory. It is well suited for the study of mesoscopic configurations like those presented in the following section where the previous method would fail.

III. STUDY OF SIMPLE DESIGNS

As a first step to understand the trade-offs involved in designing CNT-based electrically-short resonant antennas, a parametric study on m-SWCNT monopoles was undertaken [9, 12]. Indeed, if a single SWCNT is expected to slow waves down by a factor of 50 [1, 2], it should also be outlined that it presents a much too high input impedance to be connected to usual 50-ohm electronics and to radiate effectively. A SWCNT has typical resistivity of a few kΩ/μm multiplied by a length of tens to hundreds of micrometers in our application with an additional contact resistance of a few kΩ [3, 13, 14] if ohmically contacted to a metal. It is thus necessary to use multiple CNTs in parallel to reduce and tune the input impedance of this antenna.

The chosen structure is a simple quarter-wavelength monopole. It consists of a vertical metal rod over a ground plane. In our case the metal rod is replaced by a bundle of CNTs. Then we vary the number of CNTs, N_{CNT} and their length, L_{CNT}. It appears that simply adding CNTs in parallel does not work. The resonance frequency scales inversely with L_{CNT} but it shifts higher when CNTs are added in parallel thus degrading the size reduction we are after [15].

Indeed putting N_{CNT} CNTs in parallel results in dividing the overall impedance and thus the kinetic inductance by N_{CNT}: $Z_{total} = Z_{CNT}/N_{CNT} = R_{CNT}/N_{CNT} + j\omega L_k/N_{CNT}$. Neglecting the magnetic inductance and resistance, the propagation velocity along the CNTs can be written:

$$v_{p,bundle} = \frac{1}{\sqrt{LC}} \approx \frac{1}{\sqrt{L_{k,tot}C_{tot}}}. \qquad (5)$$

Moreover, because the total capacitance has relatively small variations with N_{CNT}, we obtain:

$$v_{p,bundle} \approx \sqrt{\frac{N_{CNT}}{L_k C}} = \sqrt{N_{CNT}} v_{p,CNT}. \qquad (6)$$

Hence, as a first approximation, the impedance is inversely proportional to N_{CNT} and proportional to L_{CNT}, whereas the resonance frequency is proportional to $\sqrt{N_{CNT}}$ and inversely
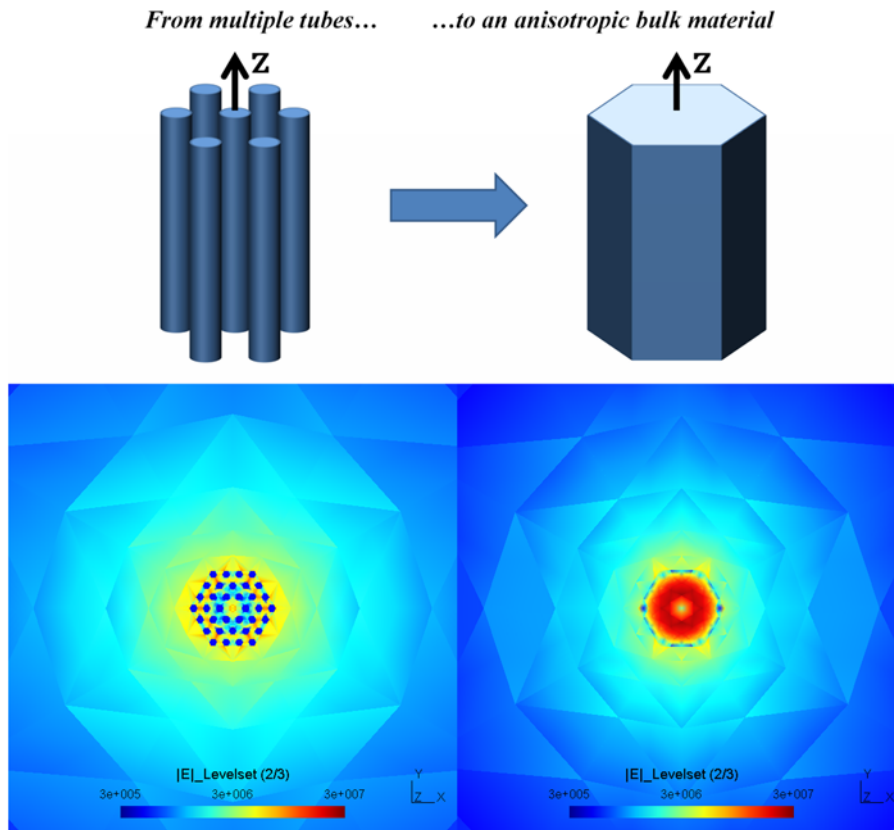
Fig. 1. Schematic illustration of the effective medium model and radial electric field distribution in a CNT monopole showing the equivalence of the hollow tube model (left) and the effective medium (right).

proportional to L_{CNT}. A trade-off thus needs to be found between size reduction, operating frequency and input impedance (cf. Fig. 2). For an antenna with good size reduction <100–1000 CNTs should be used. For it to be well-matched to 50 Ω, short CNTs thus need to be used and this leads to working at extremely high frequencies: 200 GHz and higher.

Lower frequencies and good size reduction are possible at higher impedance.

The next section describes experimental considerations and additional parametric studies led toward realizing a real electrically short resonant antenna from CNTs. The trade-offs explained here are maintained in these planar dipole structures.
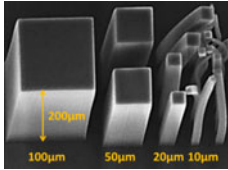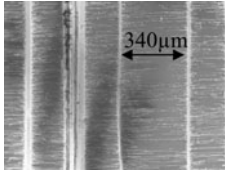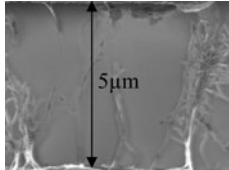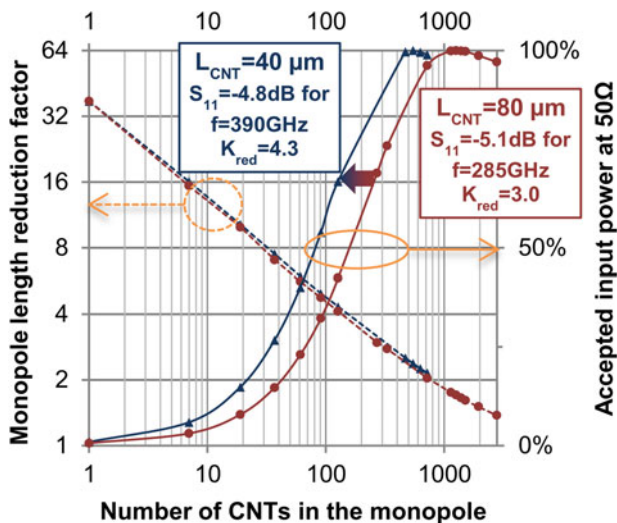
IV. EXPERIMENTALLY FEASIBLE DESIGNS

The experimental realization of these antennas is a complex task. The study presented in the previous section demonstrates the need for long high-quality SWCNTs in specific quantities which takes us to the limits of current CNT fabrication techniques. There are a few types of CNT fabrication methods, each with their particular advantages and restrictions. To observe experimentally a size reduction on a resonant antenna, these need to be considered along with simple antenna designs.

We will study monopole and dipole antennas where the axial propagation of electrons corresponds best to CNTs. The simplicity of the structure also ensures correct interpretation of the results.

As base material, three types of CNTs can be used. Dense vertical CNT arrays can be obtained by thermal (T) or plasma-enhanced (PE) chemical vapor deposition (CVD); with typical densities of 10^{10}–10^{11}/cm². Substrate-lattice-aligned horizontal CNTs can also be obtained by CVD on

Fig. 2. Illustration of the trade-offs in terms of size reduction (left), impedance match (right, the usual return loss in dB is replaced by a linear fraction of accepted power better suited to comparing slightly mismatched antennas) and resonance frequency (the two curves highlighted through the case when $S_{11}=-5$ dB)

Table 1. Different CNT types for the fabrication of an electrically short resonant antenna.

	Vertical CVD CNTs	Horizontal CVD CNTs	CNTs in solution
Illustration of typically fabricated arrays in CINTRA	PE-CVD grown MWCNT arrays on Si	TCVD grown SWCNTs on ST-cut quartz	5 μm DEP between gold electrodes
Density	$100–1000/\mu m^2$	$0.1–50/\mu m$	X (pass number for inkjet/spray)
Min(N_{CNT}) by photo-lithography	300–3000	1–100	Depends on technique
Length	10–300 μm but aspect ratio <20	5 μm–0.4 cm, dense for < 100 μm	1 μm in average, 0.1–5 μm
Quality	SWCNT only: difficult, DWCNT OK. Aligned but wavy, medium–high quality	High-quality straight to ultra-straight aligned SWCNT. Metallic-semi-conducting sorting by electrical breakdown	Random orientation.High quality, chirality/diameter sorting possible
Robustness	Bad with high aspect ratio	Excellent	Excellent
Charac-terization	*In-situ/ex-situ* (powder/large array)	*In-situ* (SEM, AFM, Raman)	*In-situ/ex-situ*
In CINTRA	Well-studied growth	Density and catalyst to improve	Buy/get CNTs; inkjet, spray, DEP, drop-casting capabilities

specific substrates such as quartz [16] then, optionally, transferred, even at wafer scale [17]; reported densities range up to $50/\mu m$ [18] but are usually from 0.1 to $10/\mu m$ – we have achieved $1/\mu m$ so far. Solution-processed CNTs can be deposited by a variety of methods rather than *in-situ* grown. Additionally photolithography is preferable for its simplicity and scalability for catalyst and electrode patterning and imposes a lower resolution limit of about 2 μm. These methods are compared in Table 1.

We conclude that only CVD-grown CNTs provide us with the necessary lengths for our application. Tunneling junction transmission through multiple solution-deposited CNTs would dampen the wave. Vertical CNTs allow the fabrication of long CNTs but, for low N_{CNT}, involve high-aspect-ratio standing structures difficult to realize. This fabrication process being well mastered in CINTRA monopole designs relying on it are under study [19]. The lattice-aligned horizontal CNTs seem to be the best logical choice with high-quality ultra-straight SWCNTs easier to connect and characterize.

The proposed design thus relies on CNTs grown by TCVD on an ST-cut quartz wafer. The first fabrication step is the patterning of metal catalyst lines. Usual lithography techniques can be used in conjunction with ebeam evaporation or spin-coating of a solution of metallic ions [20]. We adopted the technique described in [21, 22] which consists in scratching the substrate with a metallic object. CNTs are then obtained by CVD growth, before optional O_2 plasma etch of unwanted CNTs and eventually the patterning and evaporation of metal electrodes.

The proposed antenna is illustrated in Fig. 3 while the fabrication process is demonstrated by the fabrication of a CNT characterization structure: a coplanar waveguide (CPW) cut by a gap bridged by a few CNTs (Fig. 4). A CPW feed of the proposed antenna is under study. A full parametric study of the antenna has been led [23, 24]. As expected, trends similar to those of the ideal monopole arise (cf. Fig. 5): the size reduction is only dependent over the N_{CNT} used: $K_{red} \approx 50/\sqrt{N_{CNT}}$, while $f \approx (1600/L_{CNT})*\sqrt{N_{CNT}}$ and $Z_{in} \approx (400*L_{CNT})/N_{CNT}$ in (μm, GHz, Ω).

Here the study is limited to VNA measurable frequencies – up to 300 GHz. When limited to these frequencies our abacus shows that the input impedance necessarily exceeds 200 Ω for
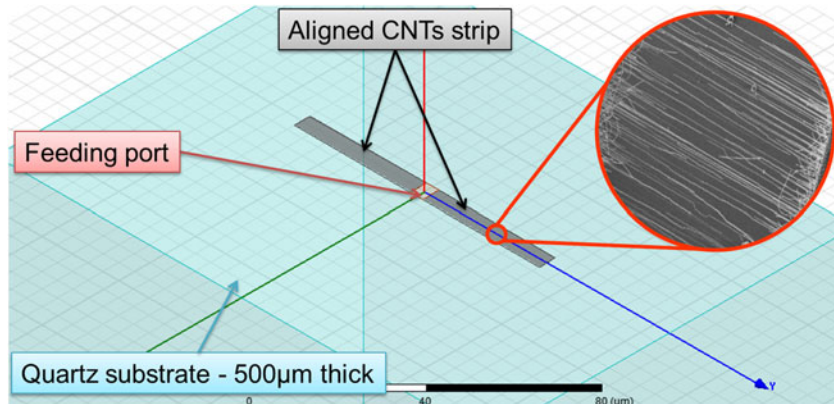
Fig. 3. CNT dipole on quartz substrate that would be realized by lattice-aligned CVD growth then O_2 plasma etching.
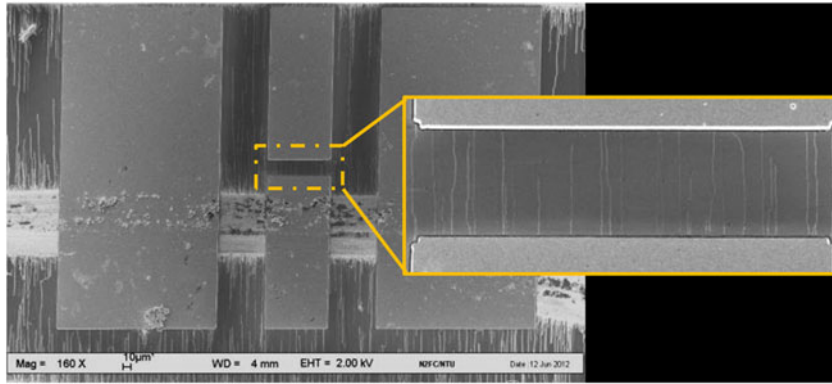
Fig. 4. Demonstration of the fabrication process by the fabrication of Au/Ti CPW gap electrodes over CVD grown CNTs.
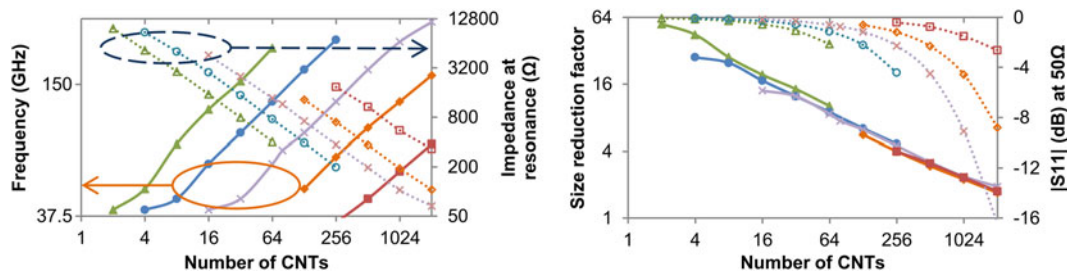

Fig. 5. Simulated characteristics of 50-Ω-fed planar SWCNT-based dipoles as a function of (N_{CNT}, L_{CNT}). (a) Resonance frequency and input impedance. (b) Size reduction and return loss. Dipole lengths are 40 (▲), 80 (●), 160 (X), 320 (◆), and 640 (■) μm with 4 μm gap.

configurations of less than 256 CNTs, which coincides with a reduction factor $K_{red} \approx 4$. Hence to operate with 50-Ω electronics at technologically relevant frequencies, one should not expect to reduce the size of their CNT resonant antenna more than four times with respect with the metal one.

Another, maybe more interesting, application of these antennas is an asymmetric wireless link acting like an impedance transformer between high-impedance nanocomponents directly connected to/incorporating an impedance-matched CNT antenna and usual microelectronics connected to a classical directive antenna [24].

V. CONCLUSION

We have described convenient simulation tools for the study of CNT-based electrically short resonant antennas. We have outlined trends and design rules as well as fabrication techniques and initial designs for these antennas. Finally, we have discussed possible applications of these antennas. They seem to be an interesting solution for the developing field of RF above 100 GHz. They can also be used to wirelessly connect high-impedance nanocomponents to conventional electronics. Design and fabrication in this direction are ongoing.

ACKNOWLEDGEMENT

REFERENCES

[1] Burke, P.J.; Li, S.; Yu, Z.: Quantitative theory of nanowire and nanotube antenna performance. IEEE Trans. Nanotechnol., **5** (4) (2006), 314–334.

[2] Hanson, G.W.: Fundamental transmitting properties of carbon nanotube antennas. IEEE Trans. Antennas Propag., **53** (11) (2005), 3426–3435.

[3] Burke, P.J.: Luttinger liquid theory as a model of the gigahertz electrical properties of carbon nanotubes. IEEE Trans. Nanotechnol., **1** (3) (2002), 129–144.

[4] Burke, P.J.: Corrections to "Luttinger Liquid Theory as a Model of the Gigahertz Electrical Properties of Carbon Nanotubes". IEEE Trans. Nanotechnol., **3** (2) (2004), 331–331.

[5] Franck, P.; Baillargeat, D.; Tay, B.K.: Mesoscopic model for the electromagnetic properties of arrays of nanotubes and nanowires: a bulk equivalent approach. IEEE Trans. Nanotechnol., **11** (5) (2012), 964–974.

[6] Slepyan, G.Y.; Maksimenko, S.A.; Lakhtakia, A.; Yevtushenko, O.; Gusakov, A.V.: Electrodynamics of carbon nanotubes: dynamic conductivity, impedance boundary conditions, and surface wave propagation. Phys. Rev. B, **60** (24) (1999), 17136.

[7] Shuba, M.V.; Slepyan, G.Y.; Maksimenko, S.A.; Thomsen, C.; Lakhtakia, A.: Theory of multiwall carbon nanotubes as waveguides and antennas in the infrared and the visible regimes. Phys. Rev. B, **79** (15) (2009), 155403.

[8] Naeemi, A.; Meindl, J.D.: Compact physical models for multiwall carbon-nanotube interconnects. IEEE Electron Device Lett., **27** (5) (2006), 338–340.

[9] Franck, P.; Baillargeat, D.; Tay, B.K.: Designing carbon-nanotube-based millimeter to sub-millimeter antennas, in IEEE Int. Topical Symp. RF Nanotechnology 2012, Singapore, 2012.

[10] Brun, C. et al.: Hybrid EM/Circuit modeling for carbon nanotubes based interconnects, Electronics Packaging Technology Conf. (EPTC) 2011, Singapore, 2011.

[11] Yang, Y. et al.: High frequency resistance of single-walled and multi-walled carbon nanotubes. Appl. Phys. Lett., **98** (2011), 093107.

[12] Franck, P.; Baillargeat, D.; Tay, B.K.: Trade-offs in designing antennas from bundled carbon nanotubes, in 2012 IEEE MTT-S Int. Microwave Symp. Digest (MTT), Montréal, Canada, 2012.

[13] Buttiker, M.; Christen, T.: Admittance and nonlinear transport in quantum wires, point contacts, and resonant tunneling barriers, in Mesoscopic Electron Transport, vol. **345**, 1997, 259–289.

[14] Lan, C.; Srisungsitthisunti, P.; Amama, P.B.; Fisher, T.S.; Xu, X.; Reifenberger, R.G.: Measurement of metal/carbon nanotube contact resistance by adjusting contact length using laser ablation. Nanotechnology, **19** (2008), 125703.

[15] Franck, P. et al.: Plasmon resonances of carbon-nanotube-based dipole antennas for nano-interconnects, in 2011 IEEE 13th Electronics Packaging Technology Conf. (EPTC), 2011, 167–170.

[16] Kocabas, C.; Shim, M.; Rogers, J.A.: Spatially selective guided growth of high-coverage arrays and random networks of single-walled carbon nanotubes and their integration into electronic devices. J. Am. Chem. Soc., **128** (14) (2006), 4540–4541.

[17] Patil, N. et al.: Wafer-scale growth and transfer of aligned single-walled carbon nanotubes. IEEE Trans. Nanotechnol., **8** (4) (2009), 498–504.

[18] Ding, L.; Yuan, D.; Liu, J.: Growth of high-density parallel arrays of long single-walled carbon nanotubes on quartz substrates. J. Am. Chem. Soc., **130** (16) (2008), 5428–5429.

[19] Brun, C.; Franck, P.; Coquet, P.; Baillargeat, D.; Tay, B.K.: Monopole antenna based on carbon nanotubes, in 2013 IEEE MTT-S Int. Microwave Symp. Digest (MTT), Seattle, USA, 2013.

[20] Zhou, W.; Rutherglen, C.; Burke, P.J.: Wafer scale synthesis of dense aligned arrays of single-walled carbon nanotubes. Nano Res., **1** (2) (2008), 158–165.

[21] Li, B. et al.: Facile "Needle-Scratching" method for fast catalyst patterns used for large-scale growth of densely aligned single-walled carbon-nanotube arrays. Small, **5** (18) (2009), 2061–2065.

[22] Cao, X. et al.: Facile "Scratching" method with common metal objects to generate large-scale catalyst patterns used for growth of single-walled carbon nanotubes. Acs. Appl. Mater. Interfaces, **1** (9) (2009), 1873–1877.

[23] Franck, P.; Baillargeat, D.; Tay, B.K.: Performance assessment of optimized carbon-nanotube-based wireless on-chip communication, in SPIE Optics and Photonics 2012: Nanoscience and Engineering, San Diego, USA, vol. **8462**, 2012.

[24] Franck, P.; Baillargeat, D.; Tay, B.K.: Design and assessment of carbon-nanotube-based remote links to nanodevices, In 2013 IEEE MTT-S Int. Microwave Symp. Digest (MTT), Seattle, USA, 2013.

Pierre Franck received the Diplôme d'Ingénieur (Master of Engineering) from Institut d'Optique Graduate School, ParisTech, Palaiseau, France in 2010 and the MSc in Applied Optics and Photonics from Imperial College London, London, United Kingdom in 2010. He worked on femto-second lasers at CEA Saclay and human-computer interaction at Imperial College. He is currently working towards the Ph.D. degree at the CNRS-International-NTU-THALES-Research-Alliance (CINTRA) in Singapore and XLIM in Limoges, France. His current interests are in design, modeling, fabrication and characterization of carbon-nanotube-based electronic and optoelectronic components with a focus on antennas.

Dominique Baillargeat received the Ph.D. degree in 1995 from the University of Limoges, France. From 1995 to 2009, he was associate professor then professor at XLIM Research Institute, University of Limoges. From 2009 to 2013, he was director of the CNRS-International-NTU-THALES-Research-Alliance (CINTRA) in Singapore. From 2013, he is director at XLIM in Limoges, France.

His research work is mainly in the following areas: (1) EM simulation and hybrid modeling coupling electromagnetic, circuits and thermal analysis, synthesis and electromagnetic optimization techniques. (2) Design and (nano)packaging of millimeter wave and optoelectronics modules, based on innovative (nano)technologies/(nano)materials. He authored or co-authored more than 150 technical papers in journals or conferences.

Prof. Baillargeat acts as expert for the French Research Agency (ANR) and French Ministry of Research . He acts as reviewer for IEEE MTT, IEEE MWCL and EuMW.

Tay Beng Kang received his degree in engineering (1985) and M.Sc. (electrical engineering, 1989) from the National University of Singapore and his Ph.D. from the Nanyang Technological University of Singapore in 1999. He became a full university professor in 2006 and is currently the Program Director for the Nanoelectronics Materials & Devices Research Group. He is concurrently holding the appointment of Associate Dean (Research), College of Engineering. NTU, Singapore.

Much of his research work has been devoted to thin film technology especially in tetrahedral amorphous carbon, metal oxides, nanocomposites and carbon nanotubes. To date, he has published more than 300 international journal papers. He is currently active in nano-engineering carbon-based hybrid systems. He is the co-inventor of 28 international patent applications. The research team was awarded the ASEAN Outstanding Engineering Award and National Technology Award in 1997 and 2000 respectively for outstanding R&D contributions on a new Filtered Cathodic Vacuum Arc Technology.